

CHANGES IN THE SURFACE LAYER OF ROLLED BEARING STEEL

Oskar ZEMČÍK^{1,*}, Josef CHLADIL², Jan OTOUPALÍK³, Josef SEDLÁK⁴

¹⁾ Ing., Ph.D., lecturer, Faculty of Mechanical Engineering, Institute of Manufacturing Technology, Brno, Czech Republic

²⁾ doc. Ing., Ph.D., lecturer, Faculty of Mechanical Engineering, Institute of Manufacturing Technology, Brno, Czech Republic

³⁾ Ing., Ph.D. student, Faculty of Mechanical Engineering, Institute of Manufacturing Technology, Brno, Czech Republic

⁴⁾ Ing., Ph.D., lecturer, Faculty of Mechanical Engineering, Institute of Manufacturing Technology, Brno, Czech Republic

Abstract: The article deals with the changes in the surface layer of the ring of rolled bearing steels. The additional method of hydrostatic roller burnishing operation is applied on samples of material 100Cr6 (EN 10132-4) and changes in the surface layer of the workpiece are then evaluated. The simulation using finite element method was used to better understand the ongoing phenomena.

Key words: bearing steel, roller burnishing, finite element method, residual austenite, residual stress

1. ROLLING TRACK OF BEARING

Roller bearings are an integral part of a large number of machines and equipment. The largest portion can be found in the automotive industry, transport machinery, machine tools, in aerospace engineering, etc. Their mechanical properties and reliability have a significant impact on the operation of the entire system. Different types of roller bearings are made from the most common ball bearings through tapered, cylindrical, and barrel bearings to special types for specific purposes. The critical point is then a dynamically loaded surface layer of the bearing ring. This ultimately leads to fatigue failure (see Fig.1 and Fig.2).

In the case of bearing rings made of bearing steel 14109 (DIN 1.3505 100Cr6) and 14209 (DIN 1.3520 100CrMn6), the layer is thermally treated, then ground and superfinished. To increase the life and reliability of the bearing there can be eventually applied the roller burnishing of dynamically loaded bearing surface layer

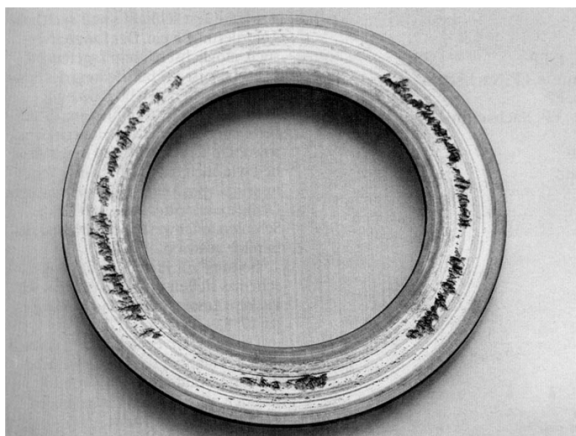


Fig. 1. Pitting on bearing ring.

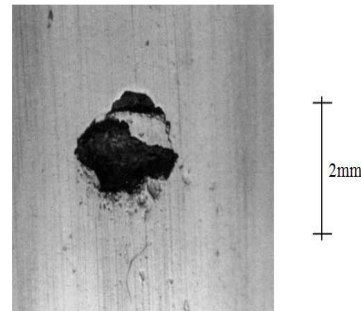


Fig. 2. Detail of pitting on bearing ring.

what brings improved properties of the ring surface layer without changing dimensions of already machined ring. This operation can also be used as additional, after pertinent dismounting of complete bearing.

2. HYDROSTATIC ROLLER BURNISHING

The method of roller burnishing does not eliminate a total residual stress induced e.g. by previous grinding, but causes compressive stresses by plastification of the surface layer [2].

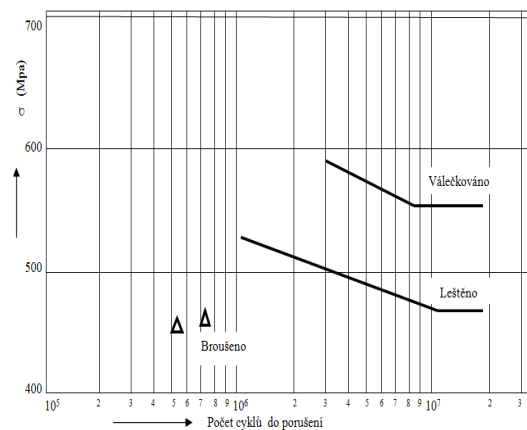


Fig. 3. Wöhler curves in samples with various surface finish [2].

* Corresponding author: Technicka 2, 61669, Brno, Czech Republic
 Tel.: 420541142409
 Fax: 420541142413
 E-mail addresses: zemcik.o@fme.vutbr.cz (O. Zemcik)

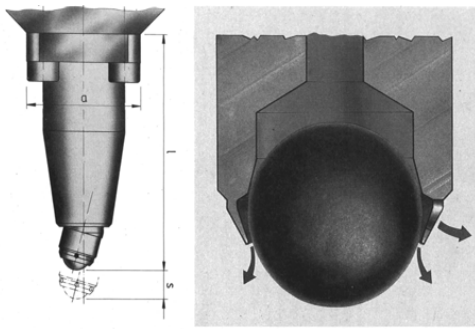


Fig. 4. Hydrostatic roller burnishing tool of company HEGENSHEIDT [8].

Compressive stresses on the surface of roller burnished area then prevent the development of cracks and eliminate the effects of micronotches.

As a roller burnishing tool in case of hardened bearing steel it is suitable to use a hydrostatic roller burnishing head with a ball-shaped element in diameter of roughly 3 mm. Hydrostatic roller burnishing heads made by company HEGENSHEIDT or ECOROLL [9] can be referred to as an example; in both cases a constant pressure of roller burnishing element on the surface of the workpiece is ensured along with the supply of process fluid to the point of contact. Convenient conditions proved to be values of speed in the range of 20–100 m.min⁻¹, feeds of 0.05 to 0.2 mm and a working force, derived from the fluid pressure of 500–2 500 N.

3. SIMULATION BY FINITE ELEMENT METHOD

To better understand the mechanism of plastic deformation in the surface layer of roller-burnished material, the simulation by means of finite element method (FEM) can be used. As a suitable candidate the ANSYS program has been selected and the simulation of stress and plastic deformations was performed in immediate vicinity of the contact point between the workpiece and the tool.

To increase the efficiency of computation, the model itself was reduced to a depth of 0.5 mm in the case of the workpiece, and the segment of ball in a length 0.3 mm.

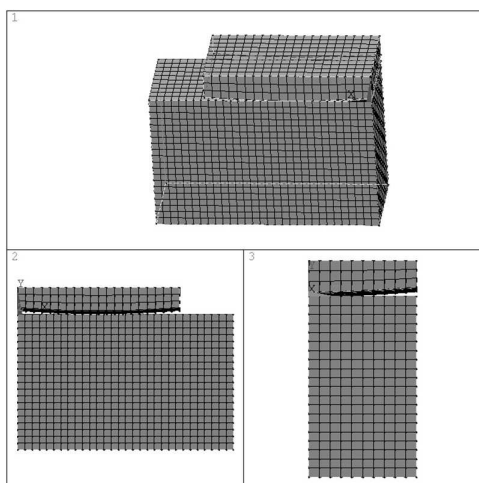


Fig. 5. Proposed 3D model for FEM.

The resultant values showed a high value of stress in the vicinity of contact point between the workpiece and the roller-burnishing element and also the formation of plastically deformed area in the surface layer as shown in the following Figs. 5 to 7.

The performed simulations show that the resultant course of stress below the roller-burnishing element is also in a relatively large extent influenced by the roller-burnishing method that was used; particularly when using a non-rolling element, a more significant plastically deformed area is shifted to the workpiece surface.

Reduced stress illustrated in Figs. 5 and 6 is defined by the relation (1) [6, 7].

$$\sigma_r = \sqrt{\frac{1}{2}[(\sigma_1 - \sigma_2)^2 + (\sigma_2 - \sigma_3)^2 + (\sigma_3 - \sigma_1)^2]} \quad (1)$$

Intensity of stress is defined by the relation (2). [6, 7]

$$\sigma_i = \text{MAX}[(\sigma_1 - \sigma_2), (\sigma_2 - \sigma_3), (\sigma_3 - \sigma_1)] \quad (2)$$

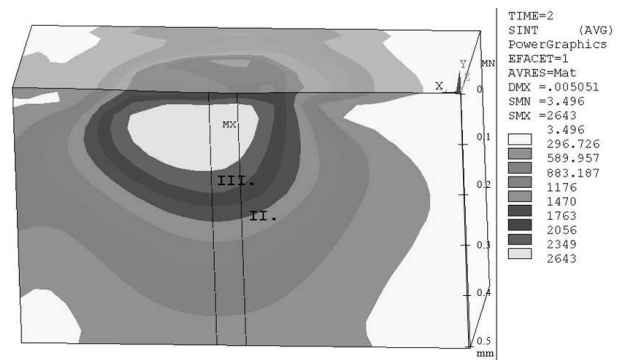


Fig. 5. 3D simulation of roller burnishing, reduced stress not affected by friction in the surface layer.

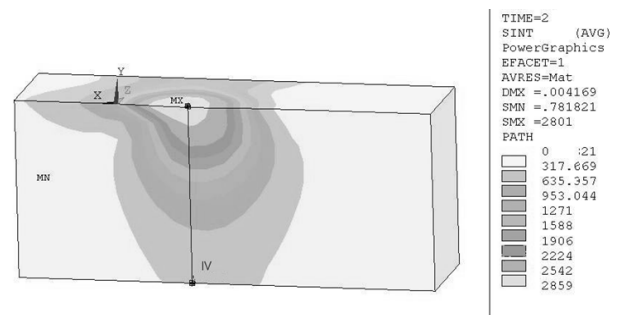


Fig. 6. 3D simulation of roller burnishing, reduced stress affected by friction in the surface layer.

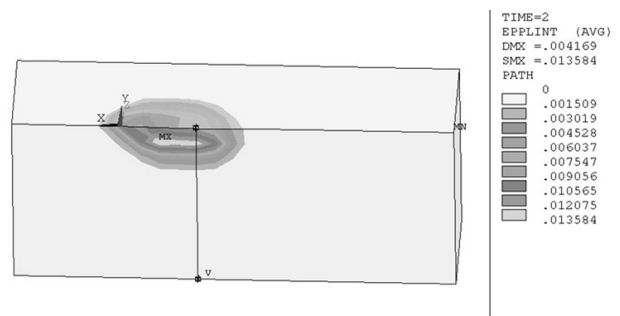


Fig. 7. 3D simulation of roller burnishing, intensity of plastic deformation affected by friction in the surface layer.

Intensity of plastic deformation is defined by the relation (3). [6, 7]

$$\epsilon_t = \text{MAX}[(\epsilon_1 - \epsilon_2), (\epsilon_2 - \epsilon_3), (\epsilon_3 - \epsilon_1)] \quad (3)$$

For better illustration of the course of plastic deformation itself in the area below the tool, it is possible to show the courses in the cross-section, as can be seen in Figs. 8 to 12.

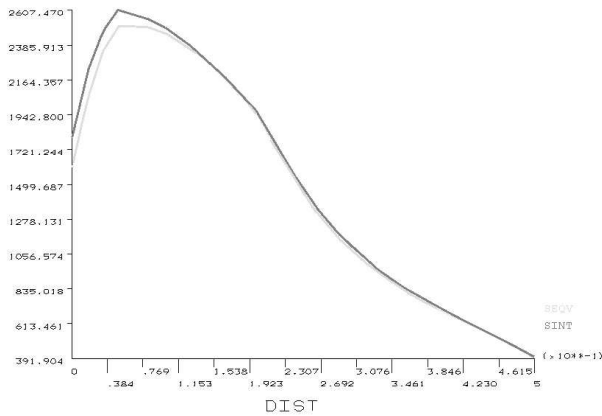


Fig. 8. Size of equivalent plastic deformation and intensity of deformation depending on the depth below the surface, cross-section III.

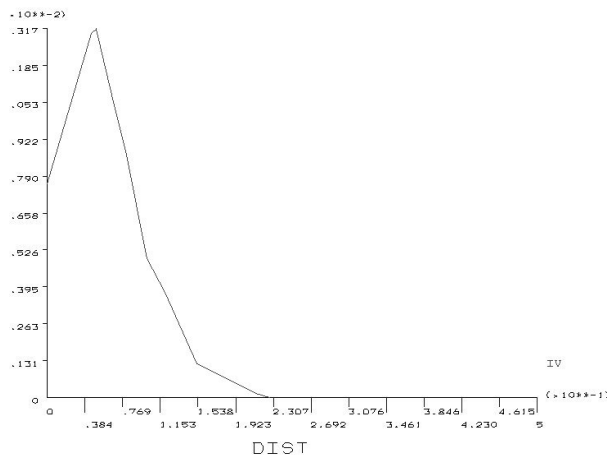


Fig. 9. Course of intensity of deformation depending on the depth below the surface, cross-section IV.

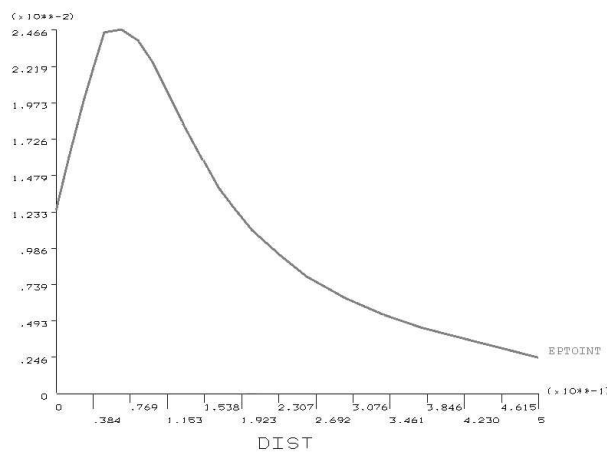


Fig. 10 Size of equivalent plastic deformation depending on the depth below the surface, cross-section IV .

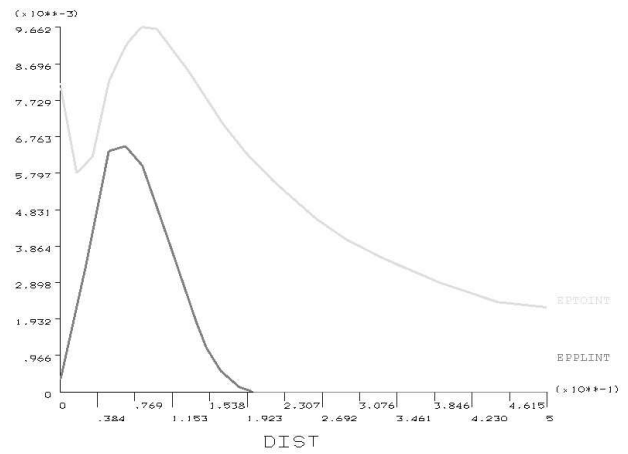


Fig. 11. Size of equivalent plastic deformation and intensity of deformation depending on the depth below the surface, cross-section II.

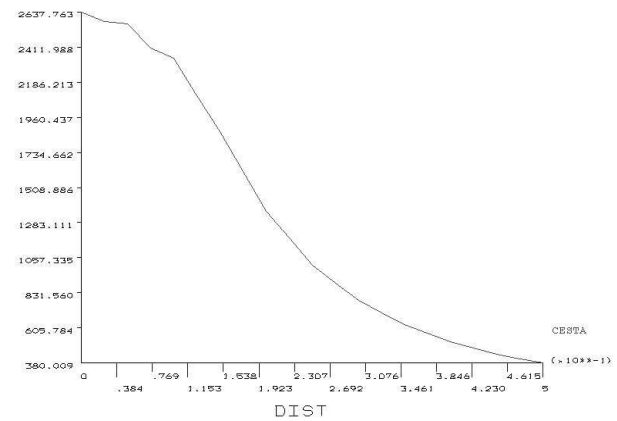


Fig. 12. Size of equivalent plastic deformation depending on the depth below the surface of the workpiece, cross-section V.

The performed simulations showed an excess of stress in the surface layer of the workpiece up to a depth of roughly 0.2 mm. This leads to plastic deformation and has a significant impact on the examined material layer.

4. PRACTICAL MEASUREMENTS

For the actual evaluation of changes in the surface layer, residual stress was measured and surface roughness of roller-burnished surface was evaluated. Next, scratch pattern was carried out in the evaluated layer and images were obtained from optical and electron microscopes.

4.1. Change in roughness

In relation to the previous simulations, different values of working force acting on the forming element were tested. The forming element, made of sintered carbide, had a diameter of 3 mm and a spherical shape. A selection of other technological parameters did not have such a major impact compared to the change in working force. Therefore, values of working speed $v_k = 30 \text{ m.s}^{-1}$ were chosen, and the feed per revolution was $f = 0.05 \text{ mm}$, which correspond to the recommended values.

Table 1
Roughness of roller-burnished surface

F[N]	Ra[μm]	Rz[μm]
100	0.048	0.6
250	0.135	0.61
500	0.118	1.09
750	0.081	0.84
1000	0.205	2.09
1500	0.291	1.41
2000	0.139	1.18
2500	0.401	2.86

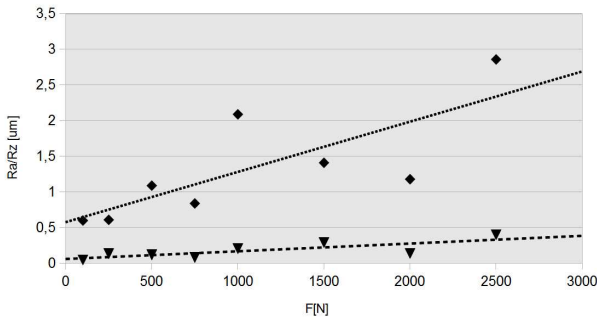


Fig. 13. Arithmetical mean roughness *Ra* and maximum height of profile *Rz* depending on the size of working force *F*.

Both the arithmetic mean roughness *Ra* and the maximum height of profile *Rz* [1] were evaluated. The values obtained are shown in Table 1.

Measurements of the individual values were repeated and mean values were entered.

From the resulting measurements, a more significant increase is clearly apparent in surface roughness with excess in the working force of 1 000–1 500 N. However, this value still meets the parameters required for the final state of the workpiece surface. Therefore, in terms of surface roughness, the optimum value of working force proved to be the value from 500 to 1 000 N.

4.2. Residual stresses in the surface layer

The value of residual stress was measured in the surface layer of the raceway of bearing ring. This ring was ground and then superfinished. The resulting value was between -250 and -350 Mpa. The negative value indicates a compressive stress in the surface layer. In case of ground surface, this value then ranged from -200 to +300 MPa. This difference is largely due to higher thermal loading of the surface layer during grinding, compared to superfinishing. To measure the residual stress values, two methods were applied. First, the mechanical method using deformation changes that result from hole-drilling at the point of measurement. This method evaluates the deformation with a strain gauge rosette placed at the measuring point.

An example of data obtained by measurement using a hole-drilling method can be seen in Figs. 14 and 15.

Furthermore, the roentgenographic method, which evaluates the crystal lattice deformation [3] in the individual phases of the material under consideration. The used equipment (Philips D500) also allowed an assessment of the percentage representation of each

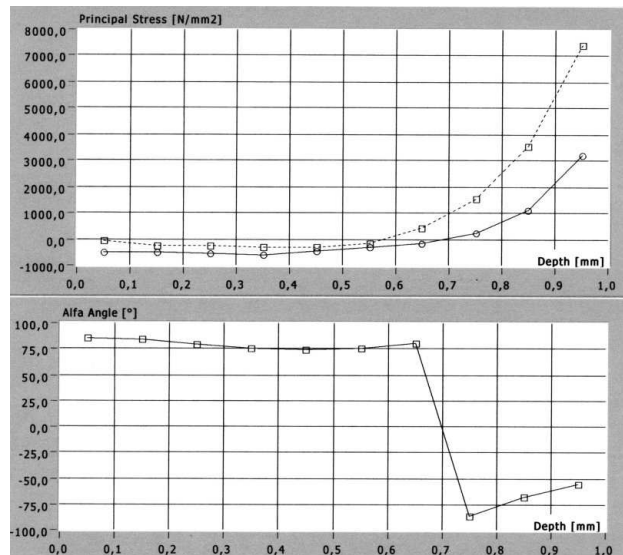


Fig. 14. Size of principal stresses depending on the depth below the surface of the outer ring of bearing PLC 46-8-2.

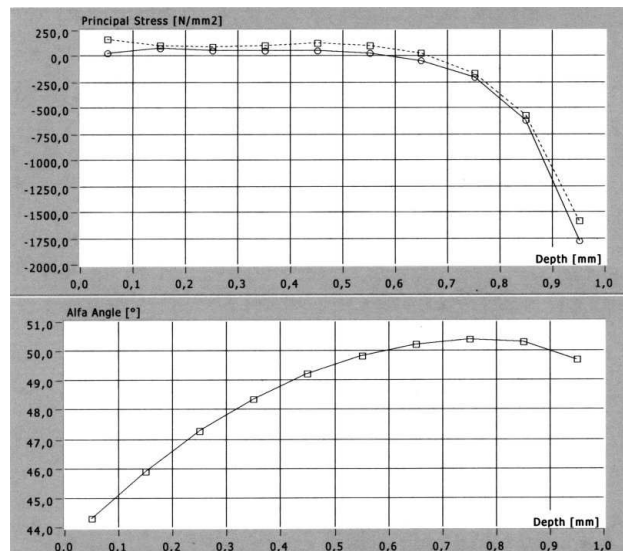


Fig. 15. Size of principal stresses depending on the depth below the surface of fine-burnished sample (steel 14109.4 HRC63).

metal phase; due to this it was possible for each measurement of residual stress to determine the amount of residual austenite in the surface layer.

The resultant value of percentage representation was measured with an accuracy of ± 1% out of the total volume of material. An example of this measurement can be seen in Fig. 16. However the depth of the layer measured by this method was limited to 40 μm below the surface.

Significantly higher values of stress in case of measuring by X-ray method can be mainly explained by a relatively shallow depth of measurement compared to a hole-drilling method where the depth amounted to a few tenths of mm.

Within the measurement, changes were then evaluated of the amount of residual austenite depending on the size of the working force and subsequently the amount of residual stress depending on the working force

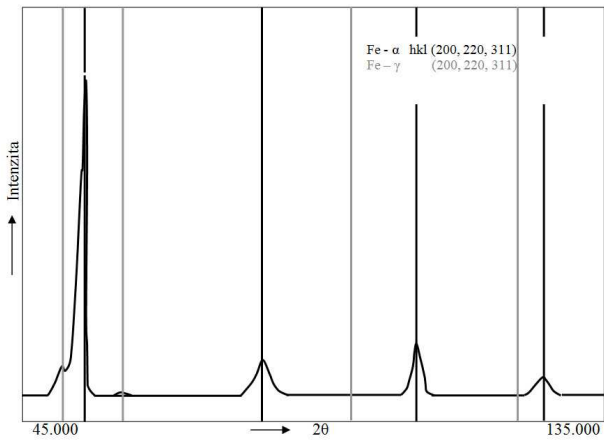


Fig. 16. Intensity of refracted X-rays depending on the angle of refraction.

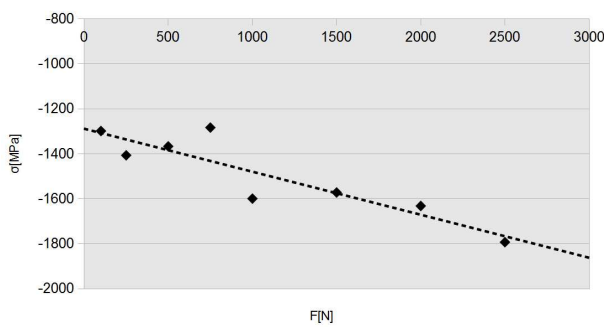


Fig. 17. Dependence of residual stress in the surface layer on the size of working force.

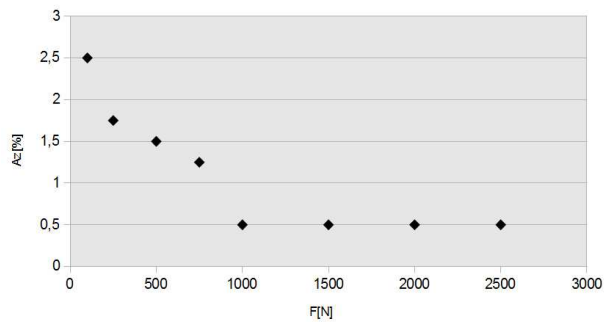


Fig.18. Dependence of the amount of residual austenite in the surface layer on the size of working force.

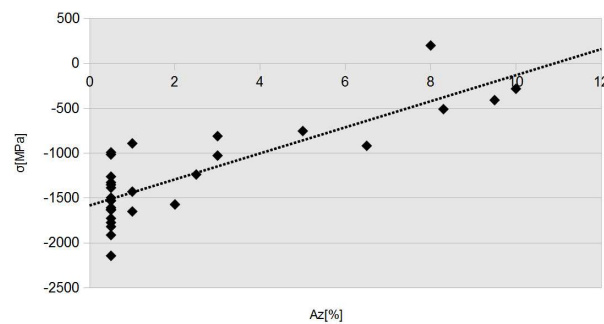


Fig. 19. Dependence of the amount of residual austenite in the surface layer on the size of working force.

was assessed. Both these dependencies are clearly seen in Figs. 17 and 18.

The rising value of pressure residual stress with increasing value of working force is, within the measured interval, approximately of linear nature.

The amount of residual austenite in the surface layer then decreases up to the working force of 1 000–1 500 N, where it reaches its minimum value.

Both these experiments led to the third dependence, i.e. the size of residual stress depending on the amount of residual austenite. This dependence enabled us to record all measured values under different technological conditions.

4.3. Structure of surface layer

For evaluation of the structure state in the surface layer, methods of light and X-ray microscopy were used. The respective steel with 1% C, 0.4 % Mn and 1.5 % Cr is used for rolling elements and rings of thickness up to 25 mm. The samples were, similarly to mass-produced rings of rolling bearings, hardened and tempered at low temperature. Between the operations of rough grinding and fine grinding, the samples were also artificially aged at temperature of 140°C for 2 hours. The assumed resulting structure consists of a very fine structure of Martensite needles evenly distributed between carbide particles. Another component is then a small amount of residual austenite which is usually located in enclosed areas between Martensite needles (see Fig. 22).

Figs. 20 to 23 show a microstructure of a roller burnished layer to a depth of a few tenths of mm. In this image, plastic deformation is clearly seen; original structures are inclined by up to 45°. To assess the possible phase changes in the surface layer, X-ray replica images were carried out at high resolution.

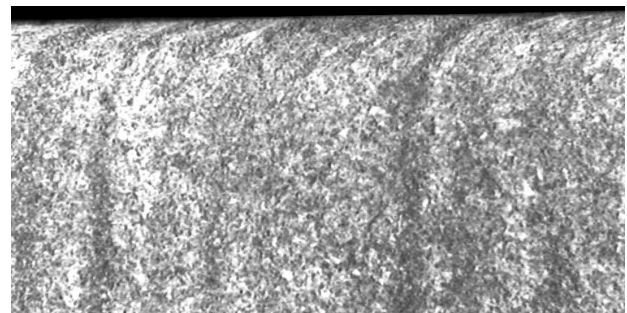


Fig. 20. Steel for roller bearings 14 109, Nital 1% 150x, roller-burnished by working force of 2 500N.

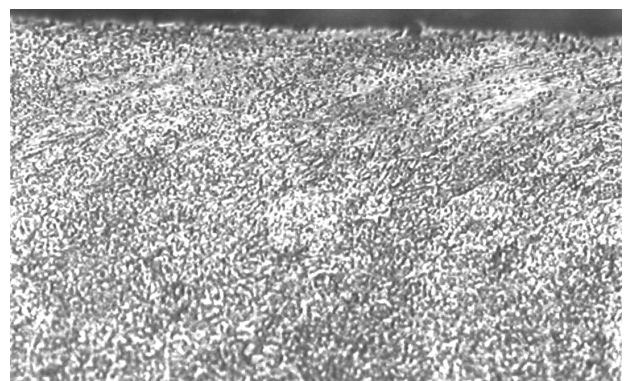


Fig. 21. Steel for roller bearings 14109, Nital 1% 750x, roller-burnished by working force of 2500N.

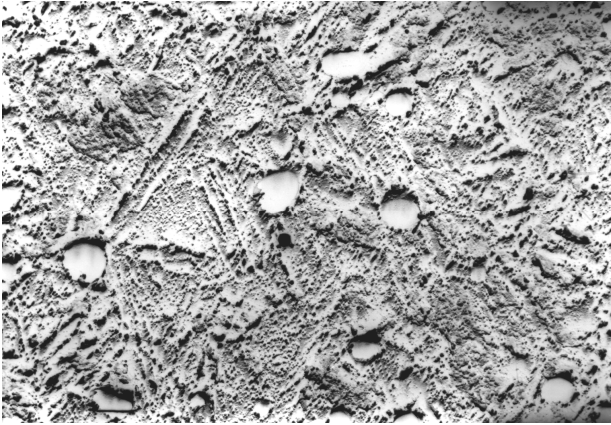


Fig. 22. Steel for roller bearings 14109.4, 10000x, roller-burnished by working force of 2500N, replica in depth of 0.2 mm below the roller-burnished surface.

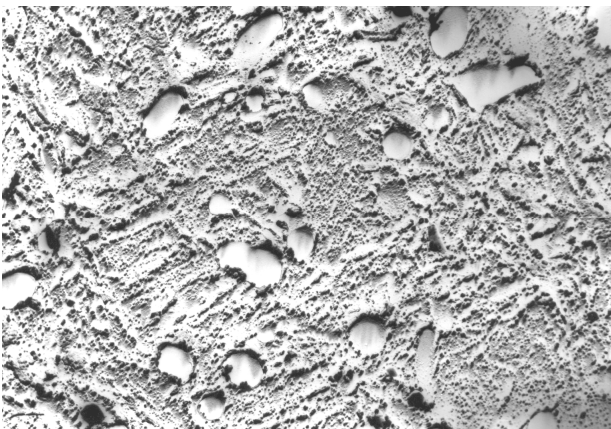


Fig. 23. Steel for roller bearings 14 109.4, 10 000x, roller-burnished by working force of 2500N, replica in depth of 0.01mm below the roller-burnished surface.

When comparing the images of the subsurface layer (Fig. 22) and the layer of a few tenths of mm below the surface (Fig. 23), a reduction of residual austenite areas is clearly seen.

5. CONCLUSIONS

The obtained results lead to the conclusion that the applied method of roller-burnishing can offer significant improvements in the properties of the surface layer of dynamically loaded bearing ring. The tested samples

showed both the improvements in the state of residual stress, and also the changes in surface layer roughness. A significant plastic deformation occurred even though the material was in a hardened state. This result may be achieved both due to plastic deformation and also due to possible phase change of the material leading to volume changes.

A positive impact on bearing life has been experimentally verified on bearings where an additional operation of roller-burnishing was applied to a rolling track; these bearings showed more than twice as long service life [5, 8]. Due to these good results in terms of surface roughness, skipping of superfinishing operation and its replacement by roller-burnishing can also be considered.

ACKNOWLEDGMENTS: The work has been supported by the Department of Trade and Industry of the Czech Republic under grant FR-TI4/247. The support gained from this source is very gratefully acknowledged.

REFERENCES

- [1] D. Paulo, *Surface Integrity in Machining*. London: Springer, 2010.
- [2] J. Vajskebr, Z. Špeta, *Dokončování a zpevňování povrchu strojních součástí válečkováním* (Finishing and surface hardening of machine parts roller), Praha: SNTL, 1984.
- [3] I. Kraus, N. Ganev, *Difrakční analýza mechaických napětí* (Diffraction stress analysis), Praha: ČVUT, 1995.
- [4] K. Vasilko, *Valivé ložiská* (Roller bearings), Bratislava: Alfa, 1988.
- [5] O. Zemčík, *Změna vlastností oběžných drah valivých ložisek po aplikaci válečkování* (Changing the properties of the grooves of rolling bearings after rolling), PhD Thesis, Brno: CERM, 2001, VUT Brno
- [6] *Ansys Theory reference: v. 13* [online], 2011, Southpointe: Ansys, Inc. [cit. 2011-07-14].
- [7] LAWRENCE, Kent L. *ANSYS Workbench Tutorial: Structural & Thermal Analysis Using the ANSYS Workbench Release 12.1 Environment*, Mission: Schroff Development Corp, 2010.
- [8] O. Zemčík, *Změna vlastností oběžných drah valivých ložisek po aplikaci válečkování* (Changing the properties of the grooves of rolling bearings after rolling), Dissertation, Brno, 2001, VUT Brno.
- [9] ECOROLL AG. *ECOROLL AG Werkzeugtechnik* [online]. Celle, 2013 [cit. 2013-05-14], available at: <http://www.ecoroll.de>